



Combined lock-in thermography and heat flow measurements for analysing heat dissipation during fatigue crack propagation

J. Bär

University of the Federal Armed Forces Munich, Institute for Materials Science, 85577 Neubiberg, Germany
juergen.baer@unibm.de

A. Vshivkov, O. Plekhov

Institute of continuous media mechanics UB RAS, 614013 Perm, Russia
poa@icmm.ru

ABSTRACT. During fatigue crack propagation experiments with constant force as well as constant stress intensity lock in thermography and heat flow measurements with a new developed peltier sensor have been performed. With lock in thermography space resolved measurements are possible and the evaluation allows to distinguish between elastic and dissipated energies. The specimens have to be coated with black paint to enhance the emissivity. The thickness of the coating influences the results and therefore quantitative measurements are problematic. The heat flow measurements are easy to perform and provide quantitative results but only integral in an area given by the used peltier element. To get comparable results the values measured with thermography were summarized in an area equivalent to that of the peltier element. The experiments with constant force show a good agreement between the thermography and the heat flow measurements. In case of the experiments with a constant stress intensity some differences become visible. Whereas the thermography measurements show a linear decrease of the signal with rising crack length, the heat flow measurements show a clearly nonlinear dependency. Obviously the measured energies in thermography and peltier based heat flow measurement are not comparable.

KEYWORDS. Fatigue; Crack propagation; Thermography; Heat dissipation.

INTRODUCTION

Lock-in thermography is widely used to gather information about the deformation behavior of metallic materials under cyclic loading. Besides elastic stress fields [1] also dissipated energies [2, 3] can be determined with this method. Therefore it can be used for crack detection [3] or for determining deformation areas around fatigue cracks [5]. Quantitative measurements are complicated due to the need of a calibration of the system and reproducible paints on the surface of the investigated specimens. A method for quantitative heat flow measurement during fatigue experiments based on Peltier elements was developed by Prokhorov et al. [6] and optimized by Vshivkov et al. [7] This method allows a simple measurement of the integral heat flow within an area specified by the dimensions of the used peltier element.

In this work the integral measurement of the heat flow with a peltier element will be combined with space resolved lock-in thermography measurements during fatigue crack propagation experiments under load as well as stress intensity controlled conditions.

EXPERIMENTAL DETAILS

Crack propagation Experiments

The crack propagation experiments were undertaken with Single Edge Notched specimens of a high-alloyed steel (X5CrNi18-10, AISI 304). SEN-specimens with a length of 80 mm and a width of 12 mm were produced from a sheet material with a thickness of 4 mm. A starter notch with a length of about 1 mm and a notch radius of 0.25 mm was machined into the specimens. Symmetrical to the notch two pins for potential drop measurement have been mounted into the specimens with a spacing of 4 mm between the pins.

The fatigue tests have been performed under fully reversed loading conditions at a frequency of 20 Hz using a servo-hydraulic testing machine with a DOLI EDC 580 controller. The machine is equipped with a specimen chamber and fixed grips to minimize bending forces. The specimen chamber is shown in Fig. 1. On the left hand side the peltier sensor for the heat flow measurement mounted from the backside is visible. On the right hand side a specimen is fitted and the peltier sensor is pressed on the backside of the specimen. A detailed description of the equipment and the test methods are given by Bär and Volpp [8].

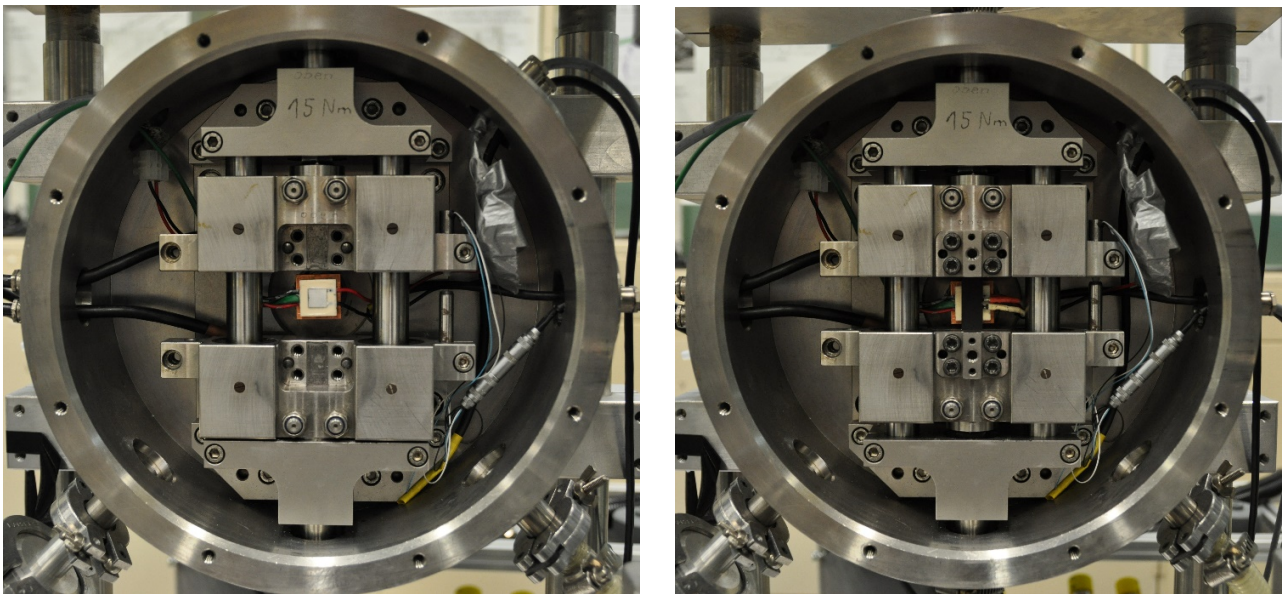


Figure 1: Specimen chamber for the crack propagation experiments. On the left image, the peltier sensor is visible. On the right the equipment with a mounted specimen is shown.

For crack length measurement a DC potential drop method was used. Therefore, a constant current of about 4.1 A was conducted through the specimen. The potential drop was measured between the two pins mounted adjacent to the notch of the SEN-specimen using an amplifier of the EDC 580 control electronics. The crack length as well as the stress intensity were calculated for each cycle and therefore it was possible to control the stress intensity during the test. Consequently, experiments with constant stress intensity K_{\max} and ΔK can be undertaken.

Thermographic measurements

The fatigue crack propagation experiments were accompanied by thermo elastic stimulated lock-in thermography. For cyclic thermal stimulation the thermoelastic effect is used in this tests. The investigations were performed with a Cedip Titanium HD 560 camera (Fig. 2) and the software Altair LI.



Figure 2: Specimen chamber with Infrared Camera.

The evaluation of the lock-in thermography is illustrated in Fig. 3. The specimen is loaded with an alternating force and the infrared camera, working with a frequency at least twice of loading frequency, records a noisy temperature signal. This temperature signal is filtered by a pixel wise fourier transformation using the frequency of the loading signal. The filtered signal shows the reaction of the specimen due to the mechanical loading. As shown on the right hand side of Fig. 3 two different values can be determined. At first the amplitude value of the filtered temperature signal and second the phase lag between the temperature curve and the mechanical loading.

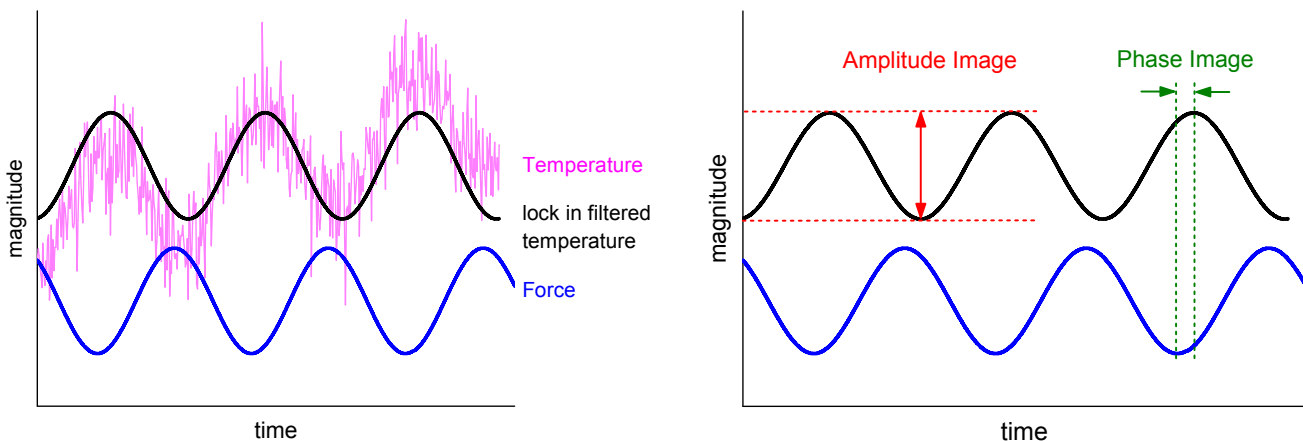


Figure 3: Lock In evaluation.

The software Altair LI delivers two different modes: the E-mode and the D-mode. The E-mode is based on the thermo elastic effect and can therefore be used for analysis of the elastic stresses as shown by Harwood et al. [9]. The D-mode provides information about the dissipated energy as shown by Brémond [10]. The software calculates the resulting amplitude of temperature variations (amplitude image) as well as the distribution of phase lags between the thermographic signal and the mechanical loading (phase image) for the E-mode and D-mode, respectively. As shown by Sakagami et al. [11] the D-Mode images can be achieved when the evaluation is performed with the double loading frequency. During the crack propagation experiments amplitude and phase images in the E- and D-Mode were received from lock-in evaluations, which were performed automatically in an defined interval of 60 s. To enhance the emissivity of the specimens the surfaces were coated with a thin graphite layer.

In Fig. 4 the resulting images of the lock in evaluation are shown. In the E-Amplitude image, the stress-field in front of the crack tip can be seen. In case of plastic deformation, the reversible adiabatic conditions are injured and therefore a phase-lag between mechanical loading and temperature signal occurs. In the E-Phase image the plastic zone can be easily identified. In the amplitude image of the D-mode a higher amplitude due to the plastic deformation is visible. In this

image also the plastic zone is clearly visible. Along the crack path also a region with a higher signal level can be seen. The latter is also visible in the D-mode phase image.

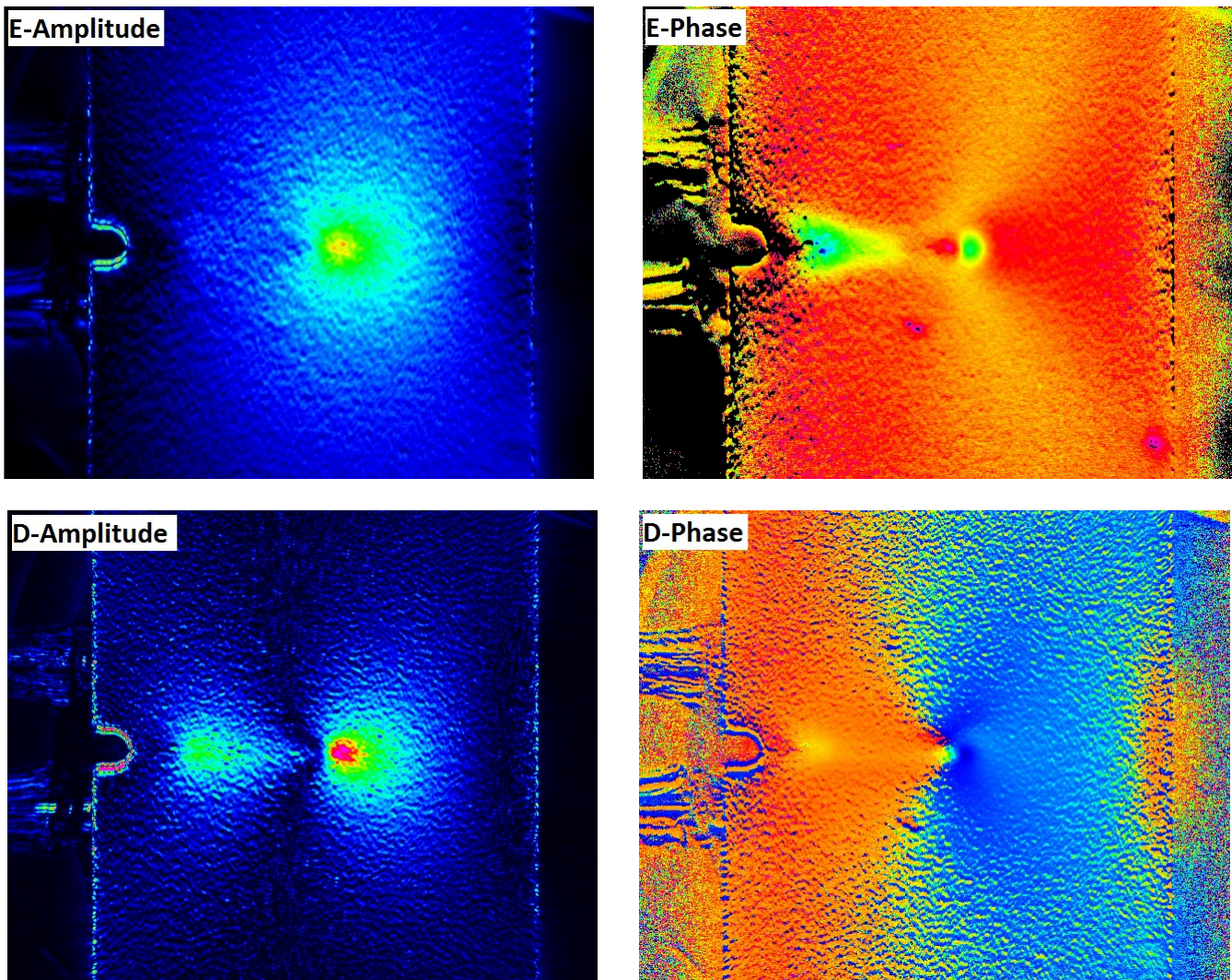


Figure 4: Evaluation of the Lock-In measurements. Left side: Amplitude pictures, right side: phase images. Upper pictures E-Mode, lower pictures D-Mode.

Heat Flow Measurements

The heat flow measurements were performed with a new developed peltier sensor. A drawing of this sensor is given in Fig. 5. The heat flow is measured by a peltier element directly attached to the specimen. To get a constant temperature on the backside of this peltier element a second peltier element is used. This second peltier element is regulated to the temperature of the chamber controlled by a thermocouple between the two peltier elements. A copper plate on the cooling peltier element ensures a good heat flow to the environment. To fix the peltier elements and the thermocouple the complete device was molded into a resin. The sensor is pressed on the backside of the specimen (Fig. 1). To enhance the heat flow, a heat-conductive paste was applied between the sensor and the specimen.

When the temperature of the specimen is changing, the corresponding temperature difference at the measuring peltier element generates a current. This current leads to a voltage at a resistor that is integrated into the electric circuit. The voltage is measured using an amplifier of the EDC 580 control electronics and is registered by the control software.

The system was calibrated with a flat resistor applicated on a plastic specimen installed into the grips. By knowledge of the voltage and the current, the power at the resistor is defined and the system can be calibrated directly to the heat flow [7].

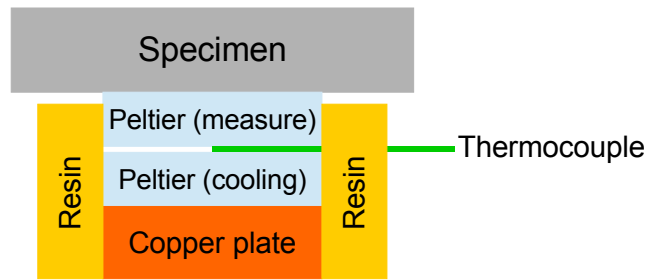


Figure 5: Schematic drawing of the peltier sensor.

RESULTS

The thermography measurement as well as the heat flow measurements were performed on force as well as stress intensity controlled experiments. The thermography measurements were performed in intervals of 60 s, i.e. 1200 cycles. For the heat flow measurement for each cycle a minimum and maximum value was acquired. To get comparable results the thermographic images were quantified by summarizing the values of all pixels in a rectangle area with size and location equivalent to that of the peltier sensor as shown in Fig. 6.

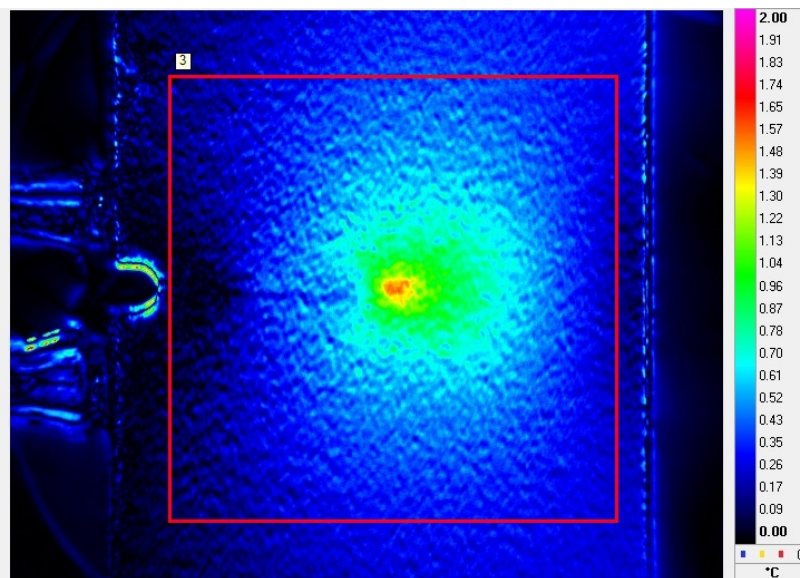


Figure 6: Evaluation of the thermographic measurements. Summation of the values of all pixels in a rectangular section of 10x10 mm.

Constant Force

In Fig. 7 the evaluation of fatigue crack propagation experiments with a constant force of 8.5 (left hand side) and 8.8 kN (right hand side) are shown. The results of the thermography measurements are drawn by symbols, the heat flow measurement is given as a solid line. It should be mentioned that in the case of the thermography measurement the assignment of the crack length to the individual measurements is not perfect, because the both measuring devices are not linked. Especially at higher crack length, i.e. higher crack propagation rates deviations may be possible although the crack length was checked with the thermography images.

In the thermography measurements, the summarized E-amplitude (blue squares) plays the dominant role. The summarized D-amplitude (red circles) is about one magnitude lower. This also reflects in the addition of the both values (black triangle) which shows nearly the same values as the E-Mode. The values of the E-mode as well as the D-mode are rising with the crack length. The only exception is the last recorded E-mode value in case of the loading with $F_{max}=8.8$ kN. This value is significant lower compared to all values determined before. On the contrary the value of the



D-mode is still rising. In case of the higher force of 8.8 kN the measured values for the E-Mode are somewhat higher compared to 8.5kN.

In both experiments undertaken with a constant force, the heat flow shows a continuous increase with increasing crack length. With rising force the curve is shifted to higher values. The slope of the curve is rising with the crack length, only at higher crack lengths of more than 7 mm the slope seems to be decreasing. At higher forces the increase of the slope is more pronounced.

The thermography measurement as well as the heat flow measurement show nearly the same behavior with increasing crack length. In case of the heat flow measurement the scatter is considerably smaller and due to the continuous measurement especially at higher crack length and therefore higher crack propagation rates more data points are available.

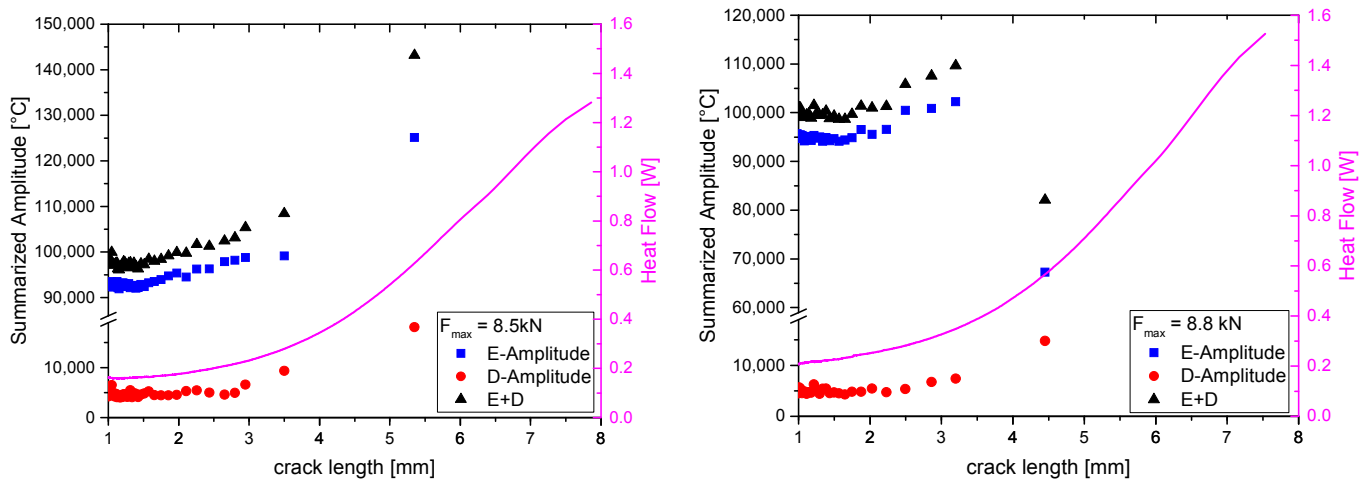


Figure 7: Evaluation of the thermographic measurements. Summation of the values of all pixels in a rectangular section of 10x10 mm.

An astonishing point in the thermographic measurement is the decrease of the summarized E-Amplitude in the last measured point in the experiment performed with 8.8 kN. The effect responsible for this decrease is visible in the last two E-Amplitude images shown in Fig. 8. On the left hand side the the second to last taken E-Amplitude image at a crack length of 3.3 mm is shown. The stress field in front of the crack tip is nearly symmetric. In the last E-Amplitude image prior to final failure, the zone in front of the crack tip is clearly asymmetric. Above the crack tip a clearly defined zone can be observed whereas below the measured amplitude is very small. The motion of the observed surface can explain this effect. Due to the high stress and the high crack length the lower part of the specimen exhibits a significant movement. The lock in evaluation is based on the analysis of the temperature change in each individual pixel. Due to the strong motion, the position of the analyzed points is changing and therefore the evaluation process is disturbed and provides incorrect values.

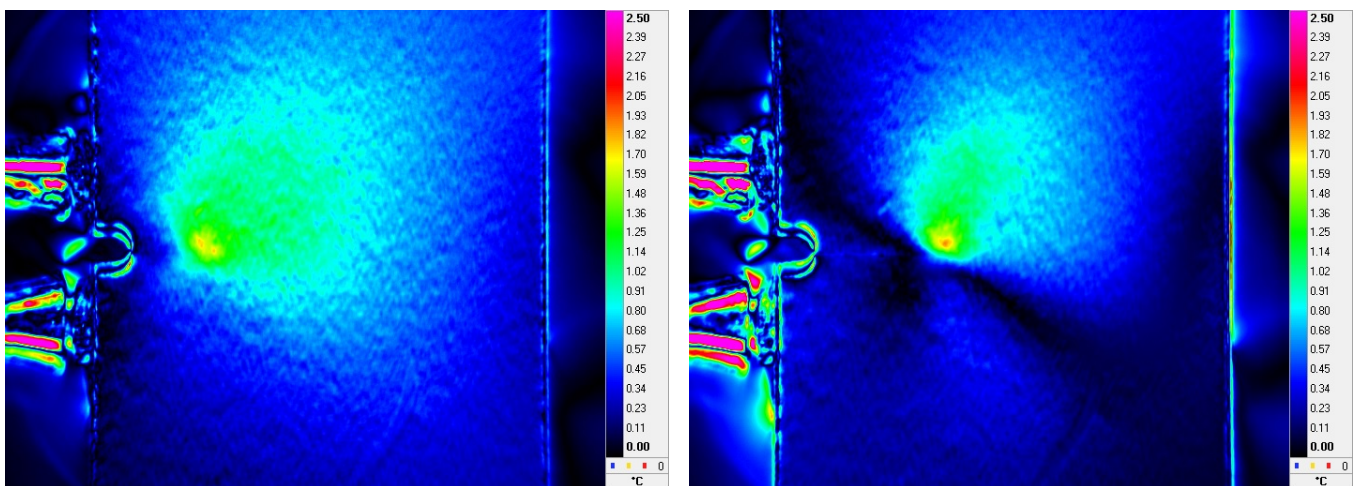


Figure 8: Second to last (left) and last E-Amplitude image received at a constant force of 8.8kN referring to Fig. 7.

In contrast to the E-amplitude the last recorded D-amplitude image shows a symmetric plastic zone in front of the crack tip (Fig. 9). An explanation for this difference may be found in the phase images. In case of the E-Mode an extreme inhomogeneous phase shift can be observed whereas in case of the D-Mode the phase shift don't show such great deviations.

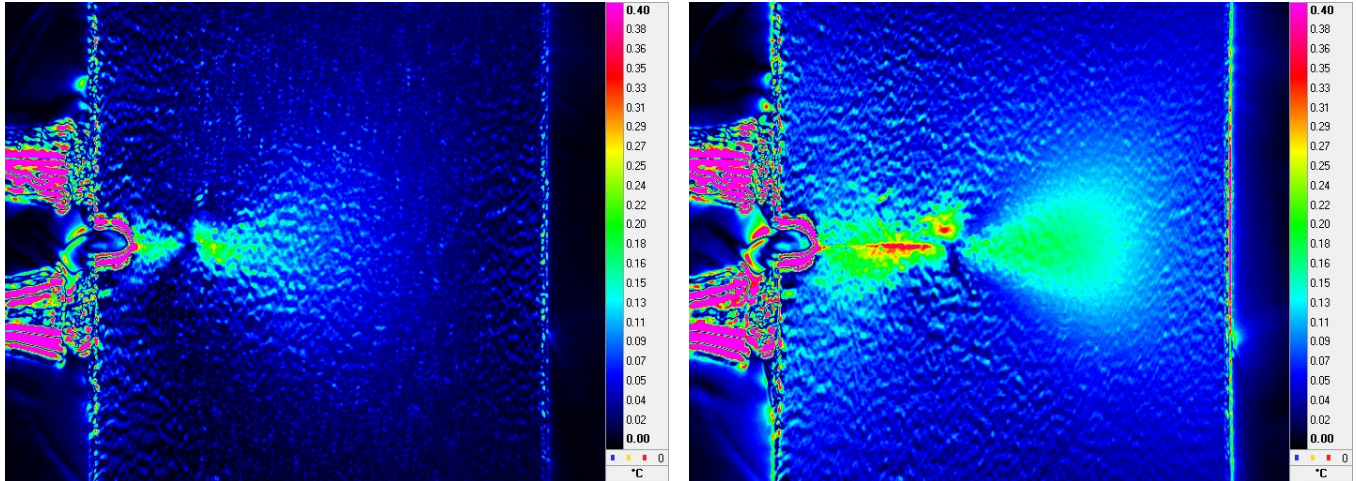


Figure 9: Second to last (left) and last D-Amplitude image received at a constant force of 8.8kN referring to Fig. 7.

Constant stress intensity

The constant stress intensity experiments were performed on loading levels of 15; 17.5; 20 and 22.5 $\text{MPa}\sqrt{\text{m}}$. The experiments consist of two phases. At the beginning, the specimen was loaded with a constant force of 8.4 to 8.8 kN until a crack was initiated and reached a length according to the desired stress intensity. Starting from this point the stress intensity K_{max} and ΔK was kept constant by reducing the force with increasing crack length.

In Fig. 10 and 11 the results of the thermography and the heat flow measurements as a function of the crack length are shown. Due to the rising crack length in phase 1 the summarized E-Amplitude as well as the heat flow is rising, too. The maximum of these curves marks the transition from constant force (phase 1) to constant stress intensity (phase 2). This peak appears in both, the thermography and the heat flow measurement, but it's more pronounced in the heat flow curve. After the peak an step decrease can be observed in the heat flow curve. The slope decreases with increasing crack length. In the Fig. 11 especially at $K_{\text{max}} = 22.5 \text{ MPa}\sqrt{\text{m}}$ steps are visible. These steps are caused by small phases with constant stress due to some small irregularities caused by the control software.

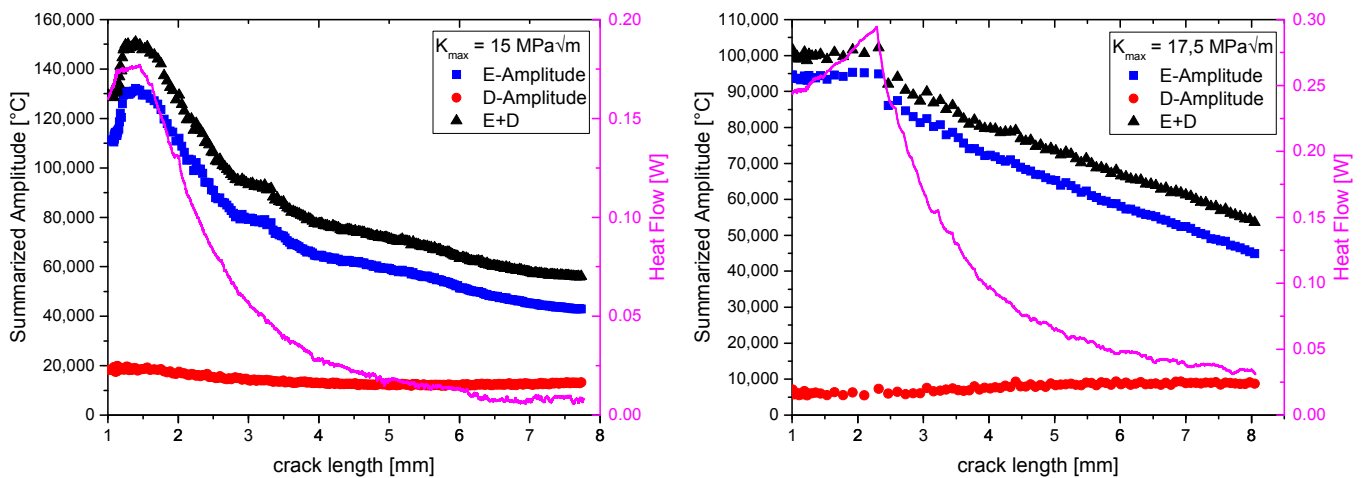


Figure 10: Experiments with constant stress intensity of 15 and 17.5 $\text{MPa}\sqrt{\text{m}}$.

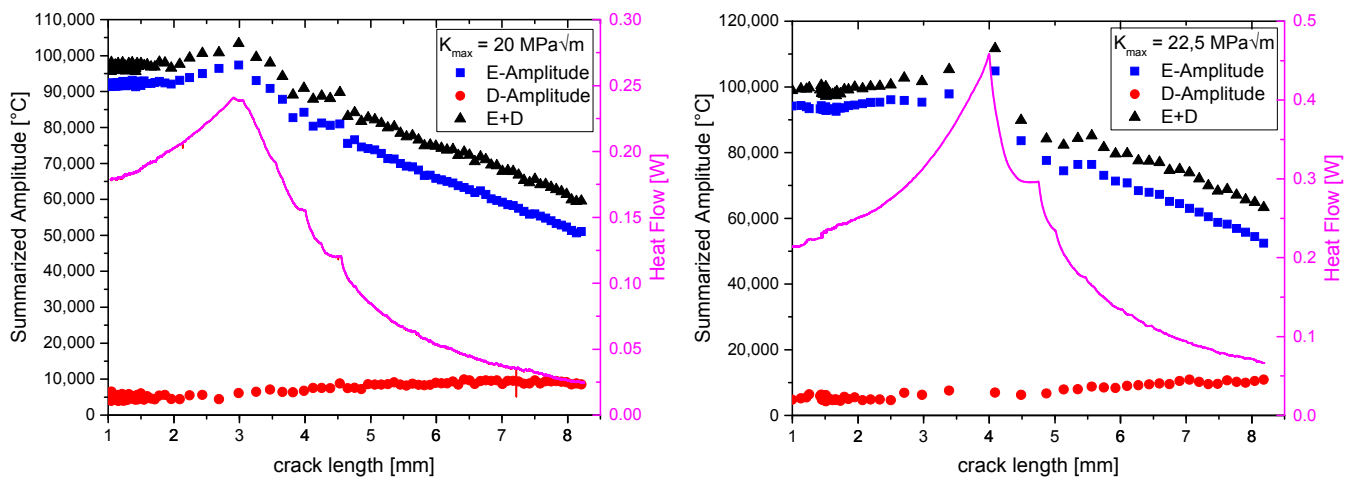


Figure 11: Experiments with constant stress intensity of 20 and 22.5 MPa√m.

In case of the thermography measurements, also a decrease of the summarized E-amplitude is visible. The slope of the decrease is considerable smaller compared than in case of the heat flow measurement. In most cases, a nearly linear decrease can be observed. In contrast to the E-Amplitude the D-Amplitude increases with the crack length. The value as well as the increase is considerable smaller, therefore the Summation of E- and D-amplitude remains decreasing with increasing crack length.

A quantitative examination of the thermography measurement shows that the specimen loaded with $K_{max}=15\text{MPa}\sqrt{\text{m}}$ shows the highest summarized E-amplitude values at the beginning of the phase with constant stress intensity. The amount of decrease is also higher in this experiment. In all other experiments, the summarized E-amplitude shows nearly the same values at the beginning of phase 2 and nearly the same decrease with increasing crack length.

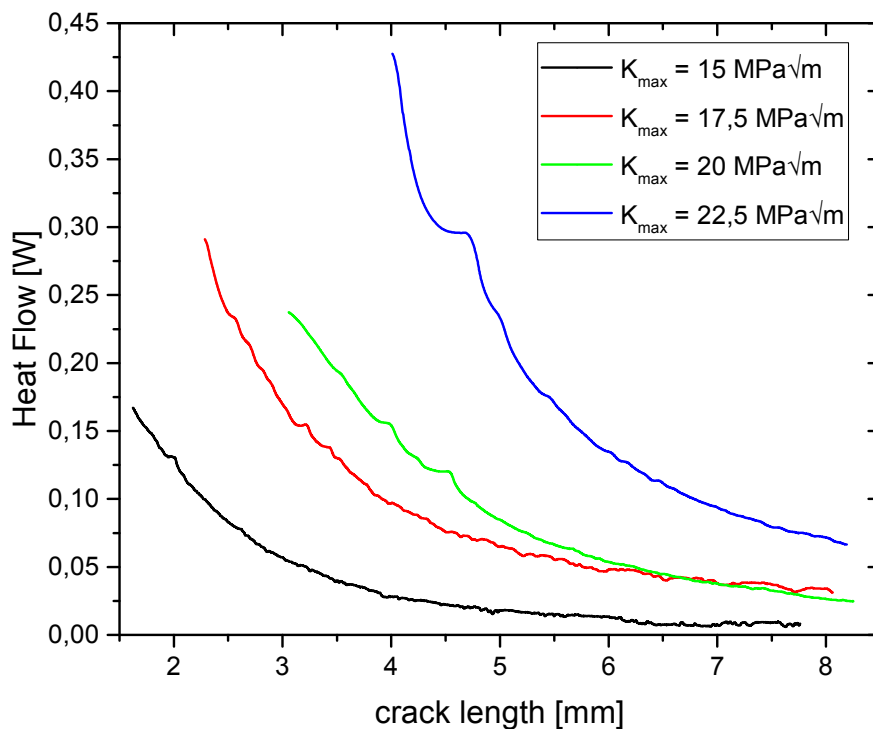


Figure 12: Heat flow experiments at different stress intensity levels.

In contrast to the thermography investigations, the heat flow measurements show a clear dependence of the applied stress intensity (Fig. 12). The measured heat flow at a given crack length is rising with the stress intensity. In addition, the

amount of decrease of the heat flow with rising crack length is also increasing with the applied stress intensity. To confirm the results some more experiments have to be undertaken.

DISCUSSION

The experiments have shown that both methods, the lock in thermography as well as the peltier element based heat flow measurement, provide interesting information about the crack propagation behavior. The lock in thermography delivers detailed space resolved information about the temperature changes due to cyclic loading. With this information, elastic stresses (E-mode) as well as dissipated energies (D-mode) can be determined qualitatively. To enhance the surface emissivity metallic specimen have to be coated with black paint. The kind of the coating as well as the thickness are influencing the results [12]. In case of thin coatings the emissivity is a combination between the specimen surface and the coating, in case of thick coating the measured response is that of the coating. Therefore, the coating of the specimen has to be done with great accurateness and the thickness has to be the same to get comparable results. In this study, a graphite spray was used as coating and was sprayed in the same manner on all specimens, but the thickness was not measured and may vary from specimen to specimen. Therefore, the results obtained on different specimen are not comparable.

With the peltier sensor it is easy to gather quantitative results during the fatigue experiments. The sensor is pressed on the specimen surface with a constant force. The thermo-paste between the sensor and the specimen enhances the heat flow and minimizes sliding effects. Consequently, it is possible to measure quantitatively but the integral measurement is limited to the dimensions of the peltier element. Small differences between the specimens can be explained by different temperatures in the chamber during the experiment. In further experiments the temperature at the backside of the measuring peltier element will be kept constant.

The experiments with constant stress intensity showed considerable differences in the run of the thermography and the heat flow measurements (Fig. 10 and 11). Except the experiment with a stress intensity of $15 \text{ MPa}\sqrt{\text{m}}$ the thermography measurements show a nearly linear decrease of the summarized amplitude with the crack length. The decrease in the heat flow measurement is clearly nonlinear. To visualize the correlation between thermography and heat flow measurement in Fig. 13 the heat flow is plotted against the summarized E- and D-Amplitude for the experiments with a constant stress intensity of $K_{\text{max}}=17.5; 20$ and $22.5 \text{ MPa}\sqrt{\text{m}}$.

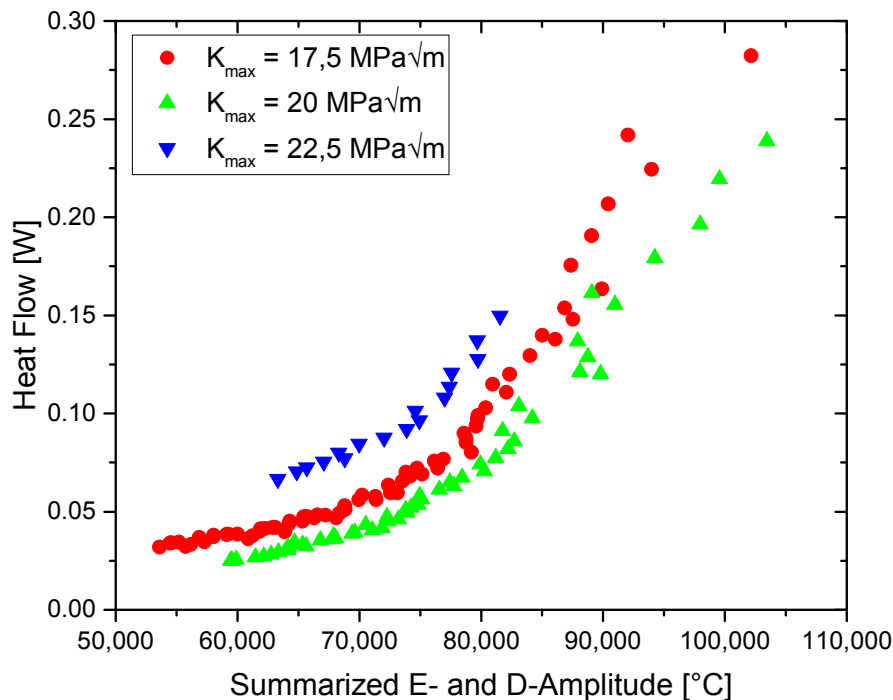


Figure 13: Heat flow experiments at different stress intensity levels.



Fig. 13 clearly shows the expected nonlinearity. All three curves show nearly the same run and are just shifted against each other. The shift can be explained by the problems to perform quantitative thermography measurements. The curves show that there is a defined correlation between the thermography and the peltier based heat flow measurement. This shows that different effects are measured with the two methods. To clarify these differences thermography measurements with defined reproducible coatings and combined heat flow measurements are projected.

The lock in thermography as well as the peltier based heat flow measurement are interesting methods to gather additional information about the crack propagation behavior of metallic materials. The lock in thermography is cost intensive, difficult to quantify and complicated to synchronize with the other data obtain in crack propagation experiments. However, this method allows space resolved measurements and can distinguish between elastic and dissipated energies. The peltier based heat flow measurement is a simple, cost-efficient method delivering quantitative results and can be easily integrated into the control electronics. Unfortunately, only integral measurements are possible. Therefore, the combination of both methods is a promising way to gather useful information about the crack propagation behavior.

ACKNOWLEDGEMENT

This work was partly supported by The Perm Regional Government № C-26/619.

REFERENCES

- [1] Díaz, F.A., Yates, J.R., Patterson, E.A., Some improvements in the analysis of fatigue cracks using thermoelasticity, *Int. J. of Fatigue*, 26 (2004) 365-376. DOI: 10.1016/j.ijfatigue.2003.08.018.
- [2] Jones, R., Pitt, S., An experimental evaluation of crack face energy dissipation, *Int. J. of Fatigue*, 28 (2006) 1716-1724. DOI: 10.1016/j.ijfatigue.2006.01.009.
- [3] Bär, J., Seifert, S., Thermographic Investigation of Fatigue Crack Propagation in a High-Alloyed Steel, *Advanced Materials Research*, 891-892 (2014) 936 – 941, DOI:10.4028/www.scientific.net/AMR.891-892.936.
- [4] Wagner, D., Ranc, N., Bathias, C., Paris, P.C., Fatigue crack initiation detection by an infrared thermography method, *Fatigue Fract. Engng. Mater. Struct.*, 33 (2009) 12–21. DOI: 10.1111/j.1460-2695.2009.01410.x.
- [5] Bär, J., Seifert, S., Investigation of Energy Dissipation and Plastic Zone Size during Fatigue Crack Propagation in a High-Alloyed Steel, *Procedia Materials Science*, 3 (2014) 408 – 413, DOI:10.1016/j.mspro.2014.06.068.
- [6] Prokhorov, A., Vshivkov, A., Iziumova, A., Plekhov, O., Batsale, J. C., Development of the measurement system for determination of energy dissipation power at fatigue crack tip, QIRT 2014-147, <http://qirt.gel.ulaval.ca/archives/qirt2014/QIRT%202014%20Papers/QIRT-2014-147.pdf>
- [7] Vshivkov, A., Bär, J., Iziumova, A., Plekhov, O., Experimental study of heat dissipation at the crack tip during fatigue crack propagation, *Frattura ed Integrità Strutturale*, (2015), in press.
- [8] Bär, J., Volpp, T., Vollautomatische Durchführung von Ermüdungsrißausbreitungsexperimenten, *Materials Testing*, 43 (2001) 242-247.
- [9] Harwood, N., Cummings, W.M., MacKenzie, A.K., An Introduction in Thermoelastic Stress in: *Thermoelastic Stress Analysis*. In: Adam Harwood, N., Cummings, W.M. (Eds.). Adam Hilger, Bristol, (1991)1 – 34.
- [10] Brémond, P., New Developments in Thermo Elastic Stress Analysis by Infrared Thermography, IV Conferencia Panamericana de END, Buenos Aires (2007).
- [11] Sakagami, T., Kubo, S., Tamura, E. Nishimura, T., Identification of plastic-zone based on double frequency lock-in thermographic temperature measurement, In: ICF11, Italy, (2005).
- [12] Robinson, A.F., Dulieu-Barton, J.M., Quinn, S., Burguete, R.L., Paint coating characterization for thermoelastic stress analysis of metallic materials, *Meas. Sci. Technol.*, 21 (2010) 085502, DOI:10.1088/0957-0233/21/8/085502.